



CHORUS

This is the accepted manuscript made available via CHORUS. The article has been published as:

Complexity at simple interfaces: Dynamically generated deep trap states at the noble-metal/alkali-halide interface

David E. Suich, Benjamin W. Caplins, Alex J. Shearer, and Charles B. Harris

Phys. Rev. B **97**, 075150 — Published 28 February 2018

DOI: [10.1103/PhysRevB.97.075150](https://doi.org/10.1103/PhysRevB.97.075150)

Complexity at Simple Interfaces: Dynamically Generated Deep Trap States at the Noble Metal/Alkali Halide Interface

David E. Suich,^{1,2} Benjamin W. Caplins,^{1,2} Alex J. Shearer,^{1,2} and Charles B. Harris^{1,2,*}

¹*Department of Chemistry, University of California at Berkeley, Berkeley, California, United States*

²*Chemical Sciences Division, Lawrence Berkeley National Laboratory, Berkeley, California, United States*

(Dated: January 29, 2018)

The trapping of delocalized electrons at ultrathin layers of NaCl on Ag(100) is investigated in real time using two-photon photoemission. Above 79 K, electrons localize to deep trap states assigned to low coordinated sites on the NaCl surface. Below 79 K, these low coordinated trap states serve as precursors for a new deep trap state at increased binding energies. The observation that the emerging trap state requires a localized precursor state suggests that a dynamic polarization of the NaCl lattice may be required for its formation. This behavior is consistent with the expectations for the formation of an interfacial (electron) small polaron which are theoretically unstable in bulk NaCl. The alkali halide/noble metal interface shows the sequential population of multiple metastable deep trap states in two-dimensions in real time.

I. INTRODUCTION

The design of molecular and nanoelectronic devices, such as transistors, memory storage, sensors, and molecular switches, requires that the active components and electrode are connected by tunneling barriers, necessitating the need for thin layer dielectrics on the nanometer scale¹. Ultrathin layers of alkali halides have been actively studied due their strong ability to decouple molecular properties from metal electrodes. This decoupling property has been demonstrated in a variety of systems. Deposition of molecules and atoms on bilayer NaCl insulating films has allowed scanning probe measurements of neutral and metastable anionic and cationic Au states^{2,3}, the isomerization of azobenzene⁴, the tautomerization of naphthalocyanine⁵, and imaging of molecular orbitals^{6,7}.

As the length scale of future electronics is reduced to the nano-regime, electron transport across the tunneling barrier will be dominated by single electron effects¹ and carrier localization will lead to charging effects in electron transport⁸. Therefore, the identification and characterization of trap states present at the dielectric interface becomes increasingly important.

The excited states dynamics of NaCl/Ag(100) are investigated using angle- and time-resolved two-photon photoemission (TPPE). TPPE is an ultrafast pump-probe technique that measures photoemitted electrons as a function of time, energy, and momentum [Fig. 1(b) inset]. This study builds upon our previous publication on NaCl/Ag(100), where the initial excited states observed were the delocalized image potential states (IPS) of the NaCl/Ag(100) interface⁹. Image potential states are a well-known class of surface states, and arise from a free electron in the vacuum inducing an attractive polarization of charges in the sample^{10,11}. In our study, the initially delocalized electrons were observed to undergo localization by trapping at defect sites on the NaCl surface. Presently, we identify a new trap state emerging at low temperatures, and characterize the timescales and energetics of the cascade of electron localization through

multiple trap states. The NaCl-noble metal interface is the first to show electron migration between multiple distinct metastable deep trap states at two dimensional interfaces in real time. The possibility that the emerging trap state observed at low temperatures is a small polaron formed via trap state intermediates is discussed.

II. EXPERIMENTAL

All experiments were performed in an UHV chamber with a base pressure $\leq 5 \times 10^{-10}$ torr. The Ag(100) surface was cleaned by standard Ar⁺ sputtering for 20 min at 500 K and annealing for 60 min at 700 K for all experiments. Three monolayer equivalents (MLE) of high purity (99.999%) anhydrous NaCl was degassed and dosed from a commercial Knudsen cell setup, with the Ag substrate held at temperature of 400 K to induce large island growth of NaCl¹² at a rate of ~ 0.3 MLE/min as described previously⁹. Supporting data of NaCl on Cu(111) is also provided. The Cu(111) substrate was held at 400 K during NaCl deposition, and low energy electron diffraction (LEED) images confirm the growth of high quality NaCl crystalline films [Fig. 4 inset]. The sample could be resistively heated or cooled with LN₂ or LHe. TPPE experiments were performed using a commercial Ti:Saph oscillator and regenerative amplifier operating at 297 kHz, which was used to pump an optical parametric amplifier (OPA). The output of the OPA provided the probe pulse, and a portion of this was frequency doubled to provide the pump with a combined cross correlation of ~ 100 fs. The energy and parallel momentum of the photoemitted electrons was detected by a time-of-flight detector.

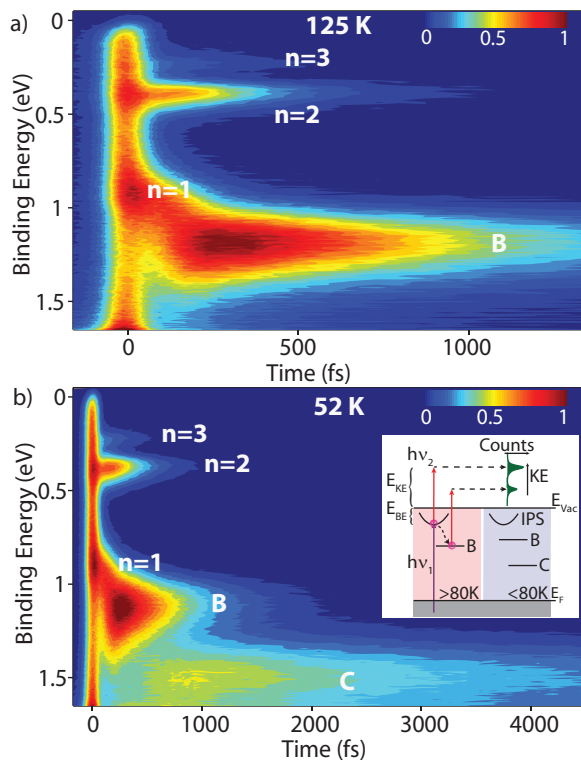


FIG. 1. (a) False color contour plot of 3 MLE NaCl on Ag(100) taken at 125 K. (b) 3 MLE NaCl at 52 K. Note the different time scales of the two plots. Inset: TPPE schematic. Pump pulse, $h\nu_1$, excites an electron to an unoccupied IPS. After a variable delay, the electron can transfer to deep trap states, and the probe pulse, $h\nu_2$, photoemits the electron, whose kinetic energy is measured via time-of-flight.

III. RESULTS AND DISCUSSION

A. Emerging Low Temperature Trap State

Deposition of 3 MLE of NaCl on Ag(100) resulted in a workfunction decrease of $\Delta\Phi = -0.58$ eV and global workfunction of 3.85 eV. For temperatures ≥ 125 K, initial excitation resulted in the population of the $n = 1, 2$, and 3 IPS. The delocalized $n = 1$ IPS electrons, as indicated by their light effective mass, m^* , of $0.7 m_e$ (relative to a free electron, $m^* = 1$), were shown to undergo a high probability of trapping due to electron transfer to the final localized state B [Fig 1(a)]. The effective mass and binding energy (BE) we reported for the $n = 1$ IPS deviate from that typically expected for IPS ($m^* \approx 1$ and a BE ≤ 0.85 eV) which is due to mixing of the $n = 1$ IPS and conduction band (CB) of NaCl^{9,13}. At 125 K, electron trapping to state B resulted in a binding energy (BE) gain of 0.34 ± 0.03 eV and an increased decay time, τ_d , of 780 fs.

The excited electron dynamics of the system significantly changes when the sample is cooled to ~ 50 K. Shown in Figure 1(b), a new state, labeled C, appears at

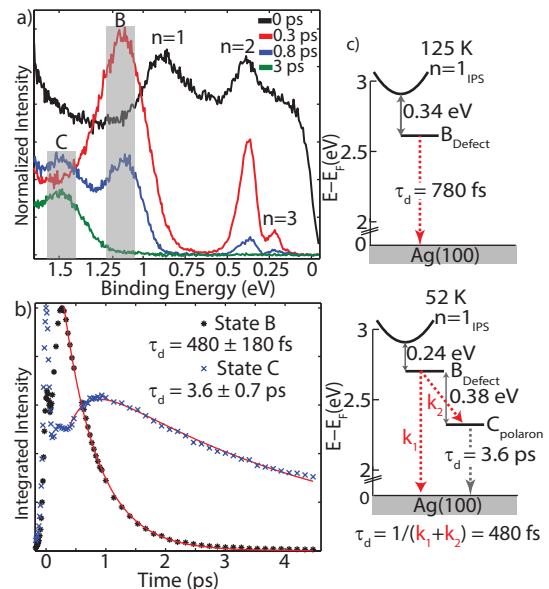


FIG. 2. (a) Time slices of Fig. 1(b). Grey boxes are 100 meV integration windows for population dynamics. (b) Population dynamics for state B and C. State B is fit to a single exponential decay, whereas state C shows a delayed exponential rise and decay. See Supporting Information for further details. (c) Summary of electron trapping and decay lifetimes at 125 K and 52 K.

long time delays and higher BE. For 3 MLE NaCl, the $n = 1$ has a BE of 0.88 ± 0.02 eV relative to E_{vac} . Electrons trapping to state B results in a BE gain of 0.24 ± 0.02 eV, and are located at a BE of 1.12 eV. This is in good agreement with the linear temperature dependent trapping energy of 1 meV/K between the $n = 1$ IPS and B observed for 125 - 350 K⁹. Further trapping to state C leads to an additional energy gain of 0.38 ± 0.02 eV to a final BE of 1.5 eV, and a combined final trapping energy of 0.62 eV. Angle-resolved measurements for state C at time delays of 0.5 and 1 ps show the state to have a flat band indicating its localized character.

Having established the trap state energetics, we now turn to the timescales of electron trapping at ~ 50 K [Fig. 2]. Electrons initially excited into the delocalized $n = 1$ IPS decay on the ~ 100 fs timescale, and localize due to population transfer to state B. Electrons trapped in state B, stabilized by 240 meV, have an increased decay time, $\tau_d = 480 \pm 180$ fs. At longer timescales (~ 500 fs), state C becomes observable, but shows a nearly order of magnitude increased $\tau_d = 3600 \pm 700$ fs compared to state B. The population dynamics of state C were fit to an exponential rise and decay, as reported in Ref. 21. The observed rise time is not intrinsic to the formation and population of state C, but rather depends on the film thickness and dosing conditions, as evidence by comparing Fig. 2(b) and Fig. 7(d). A summary of the trap state energetics and decay lifetimes are presented in Figure 2(c).

Next, we quantify the transition temperature for observing state C. Figure 3(a) shows the energetic region of state B and C at $\Delta t = 2$ ps for various temperatures. At this time delay, all IPS electrons have decayed, and only B and C are observed. At 90 K, the majority of trapped electrons reside in state B. Cooling to 80 K results in approximately equal intensity in state C and B. Finally, at 70 K, the majority of trapped electrons now reside in state C. Taking the Voigt fitted amplitude difference between state B and C at $\Delta t = 2$ ps from 60 K - 110 K, we find step like behavior [Fig. 3(b)]. Fitting this data to a sigmoid function, we extract a transition temperature, T_C , of 81 ± 8 K.

The shift in the majority of the trapped electron population from state B to C as the sample is cooled from 100 K to 60 K is coupled to the change in state B's observed decay time [Fig. 3(c)]. As the sample is cooled, state B's τ_d shows a step like decrease, and additional fitting of this trend to a sigmoid extracts $T_C = 77 \pm 8$ K. The decreasing lifetime versus decreasing temperature from 60 K - 100 K contrasts the behavior reported previously⁹ from 125 K - 350 K. Over that range, state B's τ_d exhibited Arrhenius-like behavior where τ_d increased as temperature decreased, due to thermally activated tunneling back to the metal substrate. The reversed behavior of τ_d arises from state C opening a new pathway for decay of state B in addition to decay back to the metal substrate. The two analyses of the transition temperature are in good agreement with one another and combined define $T_C = 79 \pm 8$ K. It is important to note the two measurements of the transition temperature are directly linked to each other, i.e. as the lifetime changes, the intensity at long time delays will change. However, if state

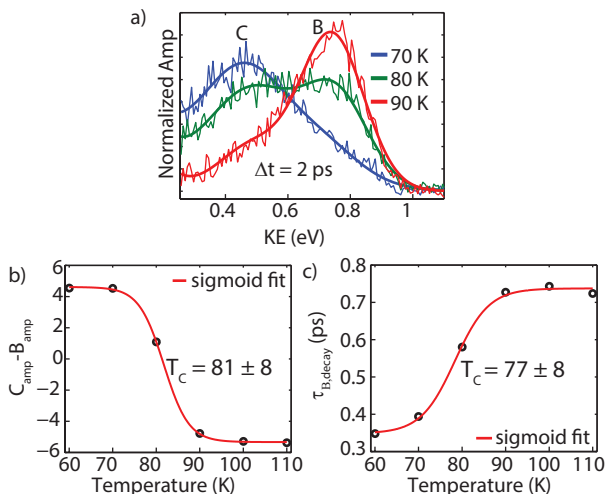


FIG. 3. (a) 3 MLE of NaCl on Ag(100) grown at a decreased dosing rate of 0.02 MLE/min. Zoom in on region of state B and C at a time delay of 2 ps for temperatures of 70, 80, and 90 K. (b) Sigmoid fit of the Voigt amplitude difference between B and C for $\Delta t = 2$ ps versus temperature. (c) Sigmoid fit to state B's τ_d versus same temperature range.

C were not populated from state B, there is no reason for this redundancy to exist. Electron transfer from state B to C is also supported by the delayed observation of C after state B intensity maximum and after the majority of the IPS electron population has decayed.

We note neither of the deep trap states observed herein have been previously identified in numerous scanning probe measurements of the NaCl/metal interface^{14–19}, which is likely due to the fact that population of the trap states B and C in our experiments are dynamical in nature and occur on ultrafast timescales making them inaccessible to scanning probe measurements that have poor time resolution. Previous reported cases of electron localization in two-dimensions, such as trapping at preexisting surface defect sites on amorphous ice²⁰, small polaron formation in alkane overlayers²¹, and solvation in thin films of acetonitrile²², observe an initially delocalized electron's wavefunction collapsing to a single localized state. Presently, we observe the cascade of electron transfer between multiple distinct trap states.

B. Comparison to Previous Studies

Trap state B is assigned to low-coordinated defect sites, such as step edges, kinks, corner sites, and NaCl pair vacancies, on the NaCl surface⁹, and further supported by dynamic force microscopy experiments which observed an increased negative tip-sample interaction at step edges and kinks relative to terrace sites¹⁴. However, assigning state C proves more difficult. Previous TPPE studies of 2-5 ML NaCl/Cu(111) by Zhu et al. in Ref. 23 assigned an electron excited into the delocalized CB and surface CB formed a small polaron, evidenced by a dynamic and continuous increase in the electron's effective mass, i.e. moving from a delocalized state to a localized state. Localization coincided with a continuous energy relaxation of 60 meV and 85 meV for the CB and surface CB, respectively, and occurred on the 100 fs timescale²³. The results in Ref. 23 are in stark contrast to ours, which shows localization to be a discrete process, i.e. distinct delocalized and localized states exist simultaneously after early time delays⁹. Additionally, localization in our experiment occurs through multiple localized states and experiences a much greater energy gain and enhanced lifetime.

To address the differences in the conclusions in our previous manuscript in Ref. 9 and this work with those in Ref. 23, we performed measurements of ultrathin layers of NaCl on Cu(111), which are shown in Figures 4 and 5. Much of spectra at early time delays is dominated by the surface states of clean Cu(111). However, after their rapid decay, the image potential state series of the NaCl interface are observed, and at longer delays a broad, long lived state at higher binding energies is observed. This is in good qualitative agreement with the electron dynamics observed for NaCl on Ag(100). Additionally, at long time delays and long integration times, the $n \geq$

4 IPS are observed [Fig. 4(b)], which demonstrates that the initial excited states of the NaCl/metal interface are predominately IPS in character rather than purely the conduction bands of NaCl. This is also in good agreement with theoretical calculations of 1-4 ML NaCl on Cu(111), which found the lowest excited states correspond to the $n = 1-3$ IPS mixed with the conduction band¹³.

For the study of NaCl on Cu(111) in Ref. 23, while the $n = 1$ IPS of clean Cu(111) was observed, the occupied Shockley state of Cu(111) was not assigned despite being energetically accessible in the experiments. Our measurements of NaCl on Cu(111) find strong energetic overlap between the surface state (SS) of Cu(111) and the $n = 2$ IPS of NaCl [Fig. 5(a-b)]. Furthermore, the choice of pump wavelength, and therefore energetic location of the virtual intermediate state of the SS, can result in an observed blue shift or red shift of the overlapping SS/ $n = 2$ spectral region. Thus, part of the energetic relaxation of the surface CB is likely due to the overlapping features. This would have additional implications for the observed continuous increase in effective mass. The Shockley state of Cu(111) has an $m^* = 0.41 m_e$ ²⁴. This feature would have the effect of causing a light effective mass observed at early time delays, which would subsequently increase as the SS decays. This partially explains the reported $m^* = 0.6 m_e$ for the surface CB and increase in effective mass in Ref. 23. Finally, we note the localization mechanism is same for our results of NaCl on Ag(100) and on Cu(111), where delocalized and localized states are observed simultaneously as shown in Fig. 5(c-d).

The electron dynamics and localization shows the same qualitative behavior for NaCl/Ag(100), KCl/Ag(100), and NaF/Ag(100) report by our group previously⁹ and also for NaCl/Cu(111), which establishes these results are generalizable. Our results for NaCl/Cu(111) and theoretical calculations serve to support the assignment of the CB and surface CB in Ref. 23 as being predominantly

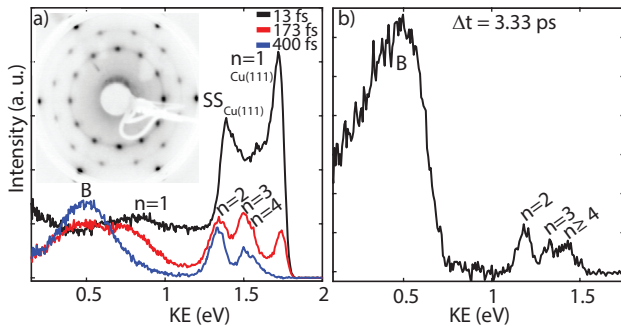


FIG. 4. (a) Time slices of ~ 2 MLE of NaCl on Cu(111) at sample temperature of 130 K and pump-probe energies of 4.13 and 2.06 eV. The Shockley surface state (SS) and $n = 1$ IPS of clean Cu(111) are identified as well as the states arising from the NaCl adsorbate. Inset: Low energy electron diffraction (LEED) image of sample at 130 K and beam energy of 62 eV. (b) Spectra of (a) at long time delay = 3.3 ps and long integration showing peaks for $n \geq 4$ IPS.

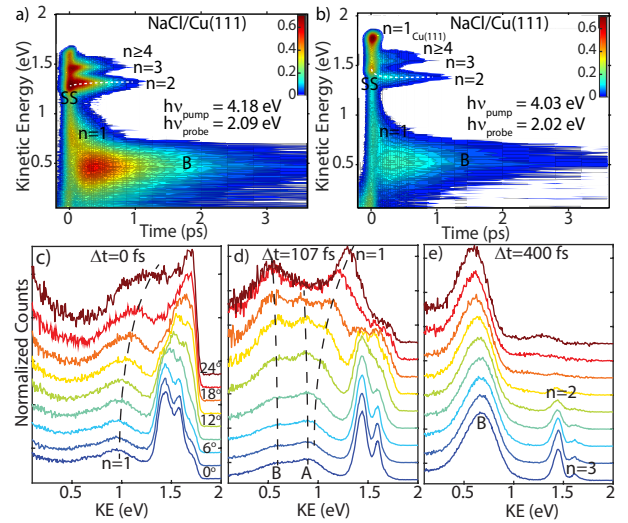


FIG. 5. (a) Log scale false color contour plots of ~ 2 MLE of NaCl on Cu(111) at a sample temperature of 130 K and pump-probe wavelengths of 4.18 eV and 2.09 eV. (b) Same as (a) but with pump-probe energies of 4.03 eV and 2.02 eV. White dotted lines serve to guide the eye to the apparent blue shift or red shift of the $n = 2$ IPS due to its overlap with the Shockley state (SS) of clean Cu(111). (c-e) Angle-resolved measurements of ~ 3 MLE NaCl on Cu(111) at pump/probe energies of 4.03/2.01 eV. The Cu substrate was held at 335 K during dosing and the spectra are taken at sample temperature of 130 K. Dispersions are taken at time delays of (c) 0, (d) 107, and (e) 400 fs. Dotted lines guide the eye to the delocalized $n = 1$ and localized states A and B.

IPS in character and more accurately assigned to the $n = 2$ and $n = 3$ IPS. While localization was observed, this is consistent with our results that the delocalized IPS localizes due to disorder in the surface potential and is accompanied by an increased BE of < 100 meV. Due to insufficient probe energy, the observation of the $n = 1$ and deep trap states were prevented in Ref. 23. The lowered substrate temperature during dosing would also likely result in a greater heterogeneous surface and the broader peak shapes observed. This establishes the initial electron localization observed in Ref. 23 most likely arises due to a disordered energetic landscape rather than small polaron formation.

C. Assigning the Emerging Trap State

One possibility for the existence of state C is a different pre-existing defect site, in which case the population of this state should be competitive with and on the same time scale as electron trapping to state B. Instead, we observe that state C forms sequentially from pre-localized electrons in state B and after the initial delocalized electrons have decayed. Charged defects, such as F-centers, require large energies to form and not present in sufficient concentration to account for the observation of

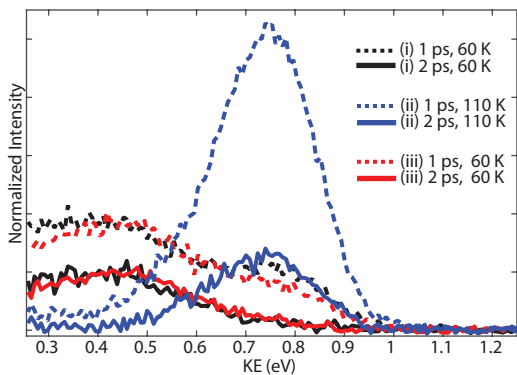


FIG. 6. Spectra of 3 MLE of NaCl on Ag(100) grown at 0.02 MLE/min at $\Delta t = 1$ (dashed) and 2 (solid) ps. (i) (black) Sample cooled to 60 K immediately after dosing. (ii) (blue) After sample in (i), the sample was flashed to 170 K for 4 minutes and cooled to 110 K. (iii) (red) Sample sequentially cooled to 60 K after (ii). Spectra are normalized to max intensity of $n=1$ at $t = 0$ ps.

state C^{25,26}.

Another possibility is that state C arises from residual gases such as water that might adsorb to the surface at low temperatures. This is highly unlikely, however, as the chamber pressure was $< 5 \times 10^{-10}$ Torr during these experiments and thus such a process should be observable on the minutes to hours timescale. Instead, we observed state C immediately upon cooling and its intensity did not grow as a function of experiment time. The reversibility of the emergence (disappearance) of state C upon cooling (heating) is shown in Fig. 6, in which a 3 MLE sample of NaCl on Ag(100) is cooled to 60 K, subsequently heated to 170 K and then cooled sequentially to 110 K and 60 K. The heating from 60 K and subsequent cooling to 60 K had no impact on state C's observed intensity. Additionally, after cooling to ca. 50 K the sample was flashed to temperatures > 175 K and immediately cooled, which had no effect on observing state C at low temperatures. This is strong evidence that state C is not the result of adsorption of residual gases.

The emerging trap state, observed for thermal energies < 7 meV (79 K), is not likely the result of any *bulk* physical change in structure, as no significant change in surface structure was observed from low-energy electron diffraction studies over the range of 25 K to 230 K²⁷. Since state C is populated from a localized state (state B) it follows that state C exists spatially in close proximity to state B. But since state C does not appear to be populated directed following excitation it is likely not a pre-existing defect (see above). Consequently, we conclude a *local* dynamic change occurs in the system allowing electrons in trap state B to evolve into state C, which can be described as the formation of a small polaron.

A small polaron arises from a charge carrier in a solid inducing a polarization and displacement of the lattice atoms resulting in an attractive potential well²⁸. Forming

a small polaron involves the competition between delocalization and localization energies, and can be expressed as,

$$E_{st} = E_{loc} - E_{rel}$$

where E_{st} is the self-trapping energy, E_{loc} is the localization energy, and E_{rel} is the lattice relaxation energy [Fig. 7(a)]²⁹. Localizing an electron residing in its lowest kinetic energy state at the bottom of a free band without lattice distortion, point F, requires the mixing of all Bloch states to form a localized wave packet, point C. The cost of localization, E_{loc} , can be approximated from half the band width ΔE . Due to the large conduction bandwidth of NaCl, electron small polaron formation is unstable in bulk NaCl^{23,30}. Localization is favored by an attractive potential well created by electron induced lattice distortion, termed E_{rel} at point S in Figure 6. Only when E_{st} is ≤ 0 is a small polaron formation stable. The rate of polaron formation will also depend on energy barriers, E_a , and transfer matrix elements between localized states.

We propose state C corresponds to the formation of a small polaron, however, we note a critical distinction

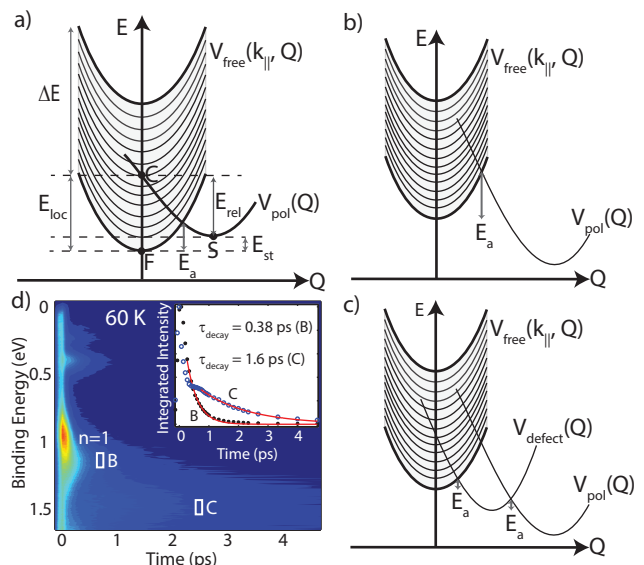


FIG. 7. (a) Adiabatic curves for electron self-trapping along lattice coordinate, Q . $V_{free}(k_{||}, Q)$ and $V_{pol}(Q)$ represent the free and polaron states, respectively. Light grey shaded curve represents distribution of free states of different $k_{||}$. ΔE represents the band width, E_{st} is the self-trapping energy, E_{loc} is the localization energy, E_{rel} is the lattice relaxation energy, and E_a is the activation energy. (b) Formation of small polaron, $V_{pol}(Q)$, directly from free electron state, $V_{free}(k_{||}, Q)$, can involve large energetic barriers. (c) Small polaron formation via localized precursor states, $V_{defect}(Q)$, can reduce the barriers to localization and forming a small polaron. (d) False color contour plots of 3 MLE of NaCl on Ag(100) grown at a dosing rate of 0.02 MLE/min. Inset: 100 meV integration normalized windows (white boxes) for trap state cross correlations and time fits.

from TPPE studies of polaron formation reported for alkanes²¹. Rather than direct formation of a small polaron from an initially delocalized state, state C only forms after electron transfer through intermediate localized states. Polaron formation in alkane thin films was supported by an analysis of the temperature and driving force dependent localization rates. The present system prevents a similar analysis because the assigned polaron is only stable at low temperatures and the precursor state is localized rather than delocalized. Theoretical calculations of an electron in deformable medium is often treated adiabatically using the Holstein model³¹. In this model, polaronic states are localized stationary states of the Hamiltonian, which can be written as $H_{tot} = H_{el} + H_{lat} + H_{int}$, where H_{el} describes an electron in a tight-binding picture, H_{lat} describes the phonons as independent oscillators, and H_{int} describes the electron-lattice interaction³². Interestingly, our results are in qualitative agreement with simulations using the Holstein model to describe electron dynamics in a 2D system which predicted self-trapping occurred through a series of intermediate localized states rather than directly from a free electron state. Localization through intermediate states was found to lower the energetic barriers to localization creating the fastest path to polaron formation³³. The combination of defect trapping and self-trapping is well established^{30,34-37}, where energetic disorder can reduce electron-phonon coupling needed to result in stable small polaron formation³⁴. Further results from the Holstein model suggest lower coordination sites, as proposed herein, facilitate the lattice deformation in electron trapping³². Thus, in the two state Marcus picture for direct electron localization via electron self-trapping, the energetic barriers (E_a) prevent the formation of a small polaron [Fig. 7(b)]. However, the presence of a third, intermediate, localized state (low-coordinated defects) can lower the barriers and enable the small polaron to be formed [Fig. 7(c)]. While we cannot directly assign the observed transition temperature (T_C) to a specific activation barrier, one possible explanation is that as temperature increases, phonon population increases, but can result in a decreased electron-phonon interaction that might prevent polaron formation³⁸.

The ability of the NaCl lattice to polarize and stabilize a negative charge has been demonstrated by the STM observation of stable Au^{-1} on a bilayer NaCl substrate and explained due to the NaCl lattice polarizing about the anion². Supporting DFT calculations found a lowering of the Au^{-1} /relaxed NaCl lattice potential energy curve of 0.53 eV relative to the neutral Au^0 /NaCl geometry³⁹, which is of a similar magnitude to our observed electron self-trapping energy of 0.38 eV. The distortion from the NaCl lattice in response to the presence of an excess electron is also supported by gas phase photoelectron studies of stable $(\text{NaCl})_n^-$ clusters ($n = 2-13$)⁴⁰. Modeling of these systems found the excess localized at corner Na^+ ions, F-center like states, or states spread over the cluster surface. However, one important feature was that all

possible modes resulted in significant deformation of the lattice to accommodate the excess electron. Although these clusters are too small to make detailed comparisons to the present work, we note that they found that the theoretical electron binding energies for the unrelaxed clusters were spread from 0.06 eV to 1.0 eV (average of 0.38 eV) depending on the cluster, which is on the same scale to the present results⁴¹.

The mechanism of small polaron formation remains an ongoing debate as to whether (i) carrier self-trapping occurs at “preexisting precursor states” or (ii) the initially excited carrier induces its own potential well in a perfect lattice⁴². Dosing 3 MLE at an order of magnitude decreased dosing rate of 0.02 MLE/min results in a loss of a pronounced rise and overall intensity loss state C’s population [Fig. 7(d)] compared with 3 MLE at a dosing rate of 0.3 MLE/min [Fig. 2(b)]. Reduction in dosing rate should result in a decrease of defect density, which results in a loss of defect precursor sites for small polaron formation. If the emerging trap state corresponded to the formation of a small polaron, this would serve to strongly support a polaron formation mechanism that only occurs at “preexisting precursor states” for the NaCl/noble metal interface.

We note the assignment of state C as the formation of small polaron is not definitive. Other mechanisms could exist, such as state C existing as a distinct pre-existing trap from state B, but which can only be populated at low temperatures due to an increased transfer matrix element between state B and C. While we believe our assignment of small polaron formation is the most plausible and supported from our data, ultimately, further detailed experimental and theoretical studies are needed to provide further insight into the nature of the emerging trap state at low temperatures.

IV. CONCLUSION

In conclusion, we used time-resolved TPPE to identify and characterize the excited state dynamics of excess electrons at the NaCl/Ag(100) interface. After initial excitation to the delocalized IPS, electrons are observed to go through a series of deep trap states. The first deep trap state is assigned to electrons trapped at low-coordinated sites on the NaCl surface such as step edges and island kinks. Below the transition temperature of 79 K, a new trap state emerges, and is tentatively assigned to small polaron formation. Unlike previous theoretical calculations that predict a delocalized conduction band electron in bulk NaCl undergoing self-trapping to be unstable, we identify a potential stable route to small polaron formation in two-dimensions. The initially delocalized $n = 1$ IPS is first trapped at defects, and then is able to form a small polaron.

ACKNOWLEDGMENTS

This work was supported by the Director, Office of Science, Office of Basic Energy Sciences, Chemical Sci-

ences Division of the U.S. Department of Energy, under Contract No. DE-AC02-05CH11231.

-
- * cbharris@berkeley.edu
- ¹ A. Tekiel, Y. Miyahara, J. M. Topple, and P. Grutter, *ACS Nano* **7**, 4683 (2013).
 - ² J. Repp, G. Meyer, F. E. Olsson, and M. Persson, *Science* **305**, 493 (2004).
 - ³ W. Steurer, J. Repp, L. Gross, I. Scivetti, M. Persson, and G. Meyer, *Phys. Rev. Lett.* **114**, 036801 (2015).
 - ⁴ A. Safiei, J. Henzl, and K. Morgenstern, *Phys. Rev. Lett.* **104**, 216102 (2010).
 - ⁵ P. Liljeroth, J. Repp, and G. Meyer, *Science* **317**, 1203 (2007).
 - ⁶ J. Repp, G. Meyer, S. M. Stojković, A. Gourdon, and C. Joachim, *Phys. Rev. Lett.* **94**, 026803 (2005).
 - ⁷ F. Mohn, L. Gross, N. Moll, and G. Meyer, *Nat. Nano.* **7**, 227 (2012).
 - ⁸ C. Brun, K. H. Müller, I. P. Hong, F. Patthey, C. Flindt, and W.-D. Schneider, *Phys. Rev. Lett.* **108**, 126802 (2012).
 - ⁹ D. E. Suich, B. W. Caplins, A. J. Shearer, and C. B. Harris, *J. Phys. Chem. Lett.* **5**, 3073 (2014).
 - ¹⁰ T. Fauster and W. Steinmann, "Chapter 8 - two-photon photoemission spectroscopy of image states," in *Photonic Probes of Surfaces*, edited by P. Halevi (Elsevier, Amsterdam, 1995) pp. 347–411.
 - ¹¹ U. Höfer, I. L. Shumay, C. Reuß, U. Thomann, W. Wal-lauer, and T. Fauster, *Science* **277**, 1480 (1997).
 - ¹² G. Cabailh, C. R. Henry, and C. Barth, *New J. Phys.* **14**, 103037 (2012).
 - ¹³ S. Díaz-Tendero, A. G. Borisov, and J.-P. Gauyacq, *Phys. Rev. B* **83**, 115453 (2011).
 - ¹⁴ R. Bennowitz, A. S. Foster, L. N. Kantorovich, M. Bamberlin, C. Loppacher, S. Schär, M. Guggisberg, E. Meyer, and A. L. Shluger, *Phys. Rev. B* **62**, 2074 (2000).
 - ¹⁵ J. Repp, S. Fölsch, G. Meyer, and K.-H. Rieder, *Phys. Rev. Lett.* **86**, 252 (2001).
 - ¹⁶ J. Repp, G. Meyer, and K.-H. Rieder, *Phys. Rev. Lett.* **92**, 036803 (2004).
 - ¹⁷ J. Repp, G. Meyer, S. Paavilainen, F. E. Olsson, and M. Persson, *Phys. Rev. Lett.* **95**, 225503 (2005).
 - ¹⁸ M. Pivetta, F. Patthey, M. Stengel, A. Baldereschi, and W.-D. Schneider, *Phys. Rev. B* **72**, 115404 (2005).
 - ¹⁹ H.-C. Ploigt, C. Brun, M. Pivetta, F. Patthey, and W.-D. Schneider, *Phys. Rev. B* **76**, 195404 (2007).
 - ²⁰ C. Gahl, U. Bovensiepen, C. Frischkorn, and M. Wolf, *Phys. Rev. Lett.* **89**, 107402 (2002).
 - ²¹ N.-H. Ge, C. M. Wong, R. L. Lingle, J. D. McNeill, K. J. Gaffney, and C. B. Harris, *Science* **279**, 202 (1998).
 - ²² A. D. Miller, I. Bezel, K. J. Gaffney, S. Garrett-Roe, S. H. Liu, P. Szymanski, and C. B. Harris, *Science* **297**, 1163 (2002).
 - ²³ M. Muntwiler and X. Y. Zhu, *Phys. Rev. Lett.* **98**, 246801 (2007).
 - ²⁴ F. Reinert, G. Nicolay, S. Schmidt, D. Ehm, and S. Hüfner, *Phys. Rev. B* **63**, 115415 (2001).
 - ²⁵ V. E. Puchin, A. L. Shluger, and N. Itoh, *Phys. Rev. B* **47**, 10760 (1993).
 - ²⁶ H. W. Etzel and J. G. Allard, *Phys. Rev. Lett.* **2**, 452 (1959).
 - ²⁷ J. Vogt, *Phys. Rev. B* **75**, 125423 (2007).
 - ²⁸ A. J. Fisher, W. Hayes, and D. S. Wallace, *J. Phys.: Con-dens. Matter* **1**, 5567 (1989).
 - ²⁹ A. L. Shluger and A. M. Stoneham, *J. Phys.: Condens. Matter* **5**, 3049 (1993).
 - ³⁰ A. M. Stoneham, J. Gavartin, A. L. Shluger, A. V. Kimmel, D. M. Ramo, H. M. Rønnow, G. Aeppli, and C. Renner, *J. Phys.: Condens. Matter* **19**, 255208 (2007).
 - ³¹ D. Emin and T. Holstein, *Phys. Rev. Lett.* **36**, 323 (1976).
 - ³² G. Kalosakas, S. Aubry, and G. P. Tsironis, *Phys. Rev. B* **58**, 3094 (1998).
 - ³³ G. Kalosakas and I. Bezel, *Chem. Phys. Lett.* **403**, 89 (2005).
 - ³⁴ D. Emin and M. N. Bussac, *Phys. Rev. B* **49**, 14290 (1994).
 - ³⁵ A. L. Shluger and J. D. Gale, *Phys. Rev. B* **54**, 962 (1996).
 - ³⁶ S. Iwai, T. Tokizaki, A. Nakamura, K. Tanimura, N. Itoh, and A. Shluger, *Phys. Rev. Lett.* **76**, 1691 (1996).
 - ³⁷ J. P. Hague, P. E. Kornilovitch, and A. S. Alexandrov, *Phys. Rev. B* **78**, 092302 (2008).
 - ³⁸ C. M. Lee, S. W. Gu, and C. C. Lam, *Physica B* **229**, 361 (1997).
 - ³⁹ I. Scivetti and M. Persson, *J. Phys.: Condens. Matter* **26**, 135003 (2014).
 - ⁴⁰ P. Xia, N. Yu, and L. A. Bloomfield, *Phys. Rev. B* **47**, 10040 (1993).
 - ⁴¹ N. Yu, P. Xia, L. A. Bloomfield, and M. Fowler, *J. Chem. Phys.* **102**, 4965 (1995).
 - ⁴² D. Muñoz Ramo, A. L. Shluger, J. L. Gavartin, and G. Bersuker, *Phys. Rev. Lett.* **99**, 155504 (2007).